Syntheses, *X*-Ray Structures, and Properties of Complexes of Macrocyclic Hexaimines with Lanthanide Nitrates†

Ata M. Arif, J. D. Julius Backer-Dirks, Colin J. Gray, F. Alan Hart,* and Michael B. Hursthouse
Department of Chemistry, Queen Mary College, Mile End Road, London E1 4NS

Complexes $[M(NO_3)_3L^1]$ {M = La or Ce, L^1 = 2,7,13,18-tetramethyl-3,6,14,17,23,24-hexa-azatricyclo[17.3.1.1^{8,12}]tetracosa-1(23),2,6,8,10,12(24),13,17,19,21-decaene}, $[M(NO_3)_2L^1(H_2O)]NO_3{\cdot}H_2O$ (M = La, Ce, or Pr), and $[\{M(NO_3)L^1(H_2O)_2\}_2]NO_3[ClO_4]_3{\cdot}4H_2O$ (M = Nd, Sm, Eu, Gd, Tb, Dy, Ho, or Er) have been synthesised by a template condensation or by ligand exchange. The *X*-ray crystal structures of a member of each series, $[La(NO_3)_3L^1]$, $[Ce(NO_3)_2L^1(H_2O)]NO_3{\cdot}H_2O$, and $[\{Nd(NO_3)L^1(H_2O)_2\}_2]NO_3[ClO_4]_3{\cdot}4H_2O$ have been determined; the complexes contain the hexadentate macrocycle L^1 co-ordinated to the lanthanide ion and are respectively 12-, 11-, and 10-co-ordinate. Properties including n.m.r. paramagnetic shifts are described.

In a preliminary report,[1] we have briefly described the synthesis of the hexaimine complexes $[M(NO_3)_3L^1]$ (M = La or Ce), together with the *X*-ray structure of the lanthanum compound. In that work, it proved impossible to obtain pure samples of analogous complexes of the heavier lanthanides by a similar synthetic method to that used for the lanthanum complex, namely the template condensation of 2,6-diacetylpyridine with ethylenediamine. The synthesis of $La(ClO_4)_3L^1(H_2O)_2$ has also been reported.[2] The template synthesis and the *X*-ray structure of a complex of the analogous ligand L^2, namely $[Sm(NO_3)(OH)L^2(H_2O)]NO_3{\cdot}2MeOH$, have been reported,[3] and here there was evidence that the initial products in the cases of the heavier lanthanides Nd, Sm, and Gd—Lu were complexes of partly hydrolysed ligands such as L^3. Use of $H_2N(CH_2)_3NH_2$ or $H_2NCHMeCH_2NH_2$ in condensation reactions with 2,6-diformylpyridine gave analogous results.[3,4] The template synthesis and properties of complexes of Ce, Pr, and Nd nitrates with the ligand L^5 have also been recently reported.[5]

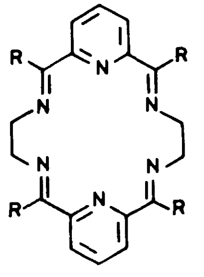

L^1 ; R = Me
L^2 ; R = H

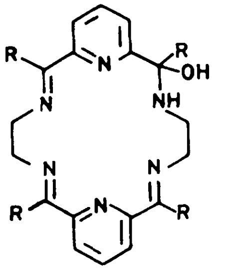

L^3 ; R = H
L^4 ; R = Me

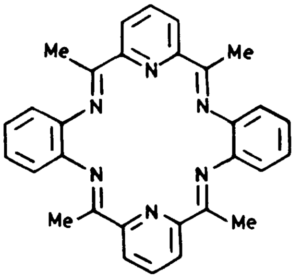

L^5

Further experiments have now established conditions under which complexes of L^1 may be obtained with lanthanides other than La or Ce. Properties and *X*-ray structures of these complexes have been determined, and together with fuller details of the structure and of the complexes originally reported,[1] form the subject of the present paper.

Results and Discussion

Preparations.—Reaction between equimolar amounts of 2,6-diacetylpyridine, ethylenediamine, and hydrated lanthanum or cerium nitrate in refluxing methanol for 4—6 h gave good yields of analytically pure crystals of $[M(NO_3)_3L^1]$ (M = La or Ce). This reaction was also attempted with heavier lanthanides (Pr—Dy) but although products were obtained, they were amorphous and i.r. spectroscopy and elemental analysis indicated that they were impure. However, it proved possible to prepare complexes of some of the heavier lanthanides by a ligand-exchange reaction. The complex[6] $[Ba(ClO_4)_2L^1]$ was suspended in an excess of aqueous lanthanide nitrate. It slowly dissolved and crystals of the hexaimine complex of the lanthanide were deposited. Two types of complex were formed: $[M(NO_3)_2L^1(H_2O)]NO_3{\cdot}H_2O$ (M = La, Ce, or Pr) and $[\{M(NO_3)L^1(H_2O)_2\}_2]NO_3[ClO_4]_3{\cdot}4H_2O$ (M = Nd, Sm, Eu, Gd, Tb, Dy, Ho, or Er). No pure crystalline products were obtained from metal replacement reactions attempted using thulium or ytterbium nitrates. The complexes had colours characteristic of the hydrated ions except for $[La(NO_3)_3L^1]$ (pale pink-brown), $[Ce(NO_3)_3L^1]$ (deep yellow), and $[Ce(NO_3)_2L^1(H_2O)]NO_3{\cdot}H_2O$ (orange). The deep yellow or orange colour of Ce^{3+} when co-ordinated to a conjugated system has been noted previously.[7] It is probably due to an essentially $f \longrightarrow \pi^*$ transition.

Properties of the Complexes.—The method of preparation involving metal transfer in aqueous solution shows that these hexaimine complexes are stable in water, in contrast to the 18-crown-6 ether (1,4,7,10,13,16-hexa-oxacyclo-octadecane) derivatives.[8] They are in fact also kinetically stable against ligand–

---

† *Supplementary data available* (No. SUP 56674, 2 pp.): cell dimensions. See Instructions for Authors, *J. Chem. Soc., Dalton Trans.*, 1987, Issue 1, pp. xvii—xx.

lanthanide ion exchange, once formed. Thus the n.m.r. spectrum of $[La(NO_3)_3L^1]$ in D_2O is unaltered for 24 h after the addition of Ce^{3+}. Similarly, the n.m.r. spectrum of $[Ce(NO_3)_3L^1]$ is unaltered by the addition of La^{3+}. Xylenol Orange, which forms a characteristic deep pink complex with lanthanide ions in aqueous solution, fails to give that colour when treated with the lanthanide complexes of L^1, showing they are inert to ligand replacement by this dye. Conductivity measurements show that dissociation of the nitrate ions occurs in aqueous solution; thus the constitution in water is $[ML^1(H_2O)_x]^{3+}$. In 0.001 mol dm^{-3} aqueous solution, $[La(NO_3)_3L^1]$ and $[Ce(NO_3)_3L^1]$ have molar conductances of 328 and 341 ohm^{-1} cm^2 mol^{-1} respectively. The corresponding value for $LaCl_3$ is 411 ohm^{-1} cm^2 mol^{-1}.

The complexes are remarkably inert towards hydroxide or fluoride ions. Thus $[Pr(NO_3)_2L^1(H_2O)]NO_3{\cdot}H_2O$ as a 0.005 mol dm^{-3} solution in 0.05 mol dm^{-3} KOH is stable for 10 min before slow precipitation of $Pr(OH)_3$ begins. A comparable experiment in which KF was used instead of KOH gave no precipitation of PrF_3 in 15 min. In comparison, similar experiments with $[Pr(NO_3)_3(18\text{-crown-}6)]$ gave instant precipitates. These hexaimine complexes therefore resemble the lanthanide cryptates, ethylenediaminetetra-acetate complexes, and complexes of sulphonated phthalocyanines and porphyrins in being stable in water; the last two ligands give complexes which are also stable towards base.

Both the anhydrous complexes $[M(NO_3)_3L^1]$ (M = La or Ce) are thermally stable up to 240 °C when they decompose rapidly. Thermogravimetric studies of $[Pr(NO_3)_2L^1(H_2O)]$-$NO_3{\cdot}H_2O$ show a weight loss of all the water by 140 °C (loss found, 4.4; calculated loss, 4.9%). This occurs in two distinct stages, 1.2% being lost by 80 °C. Similar behaviour is shown by $[\{Eu(NO_3)L^1(H_2O)_2\}_2]NO_3[ClO_4]_3{\cdot}4H_2O$, 1.6% being lost by 60 °C and 4.4% by 140 °C (calculated for total water loss, 4.9%). The Pr and Eu complexes both decompose violently at 300 °C. It is likely that lattice water is lost in the first stage of heating, followed by the co-ordinated water.

No useful mass spectra could be obtained by electron impact. No peaks were observed below decomposition temperatures and no molecular-ion peaks were obtained of either the complexes or the dissociated ligand.

The i.r. spectra are much as expected. Thus there are no bands which could be assigned to N–H or C=O modes of the unchanged reactants, but strong bands appear at 1 668—1 630 cm^{-1} due to C=N, and at 1 585—1 588 cm^{-1} due to C_5H_5N, the exact frequencies depending on the particular complex. In all three types of complex, bands indicative of co-ordinated nitrate are present in the regions 1 411—1 450 cm^{-1} and 1 293—1 340 cm^{-1}. Ligand bands occur in the region of the E' stretching mode of the unco-ordinated nitrate ion, but there are bands at 1 383, 1 371, and 1 352 cm^{-1} in the spectrum of the hydrated La complex, and at 1 378 cm^{-1} for the hydrated Sm complex. These bands may probably be assigned to this mode, which is expected to be affected by hydrogen bonding taking place to water molecules. Perchlorate bands at 1 080 cm^{-1} (broad but unsplit) and 630 cm^{-1} are consistent with unco-ordinated perchlorate ion in $[\{Sm(NO_3)L^1(H_2O)_2\}_2]NO_3[ClO_4]_3{\cdot}4H_2O$. The bands in the H–O–H bending region (1 640 cm^{-1}) are obscured by ligand C=N bands. The dihydrates $[M(NO_3)_2L^1(H_2O)]NO_3{\cdot}H_2O$ show two pairs of bands, at 3 530 and 3 500 cm^{-1}, and at 3 350 and 3 260 cm^{-1}. The broader, lower frequency, pair may tentatively be assigned to co-ordinated water as they closely resemble the corresponding absorption in $[M(NO_3)_3$-$(H_2O)_3]{\cdot}18\text{-crown-}6$.[8] The other pair would then be assigned to lattice water. It is impossible to distinguish between co-ordinated and lattice water in $[\{M(NO_3)L^1(H_2O)_2\}_2]NO_3$-$[ClO_4]_3{\cdot}4H_2O$, as the absorption is broad and strong.

The u.v. spectrum of $[La(NO_3)_3L^1]$ in aqueous solution has bands at 297 and 242 nm. These show a bathochromic shift relative to 1,2-bis(2′-pyridylmethyleneamino)ethane, a comparable molecule which has however only one instead of two C=N groups conjugated with the pyridine ring. This result disproves the possibility that a significant proportion of the >C=N– groups hydrolyse in solution to a form such as L^4.

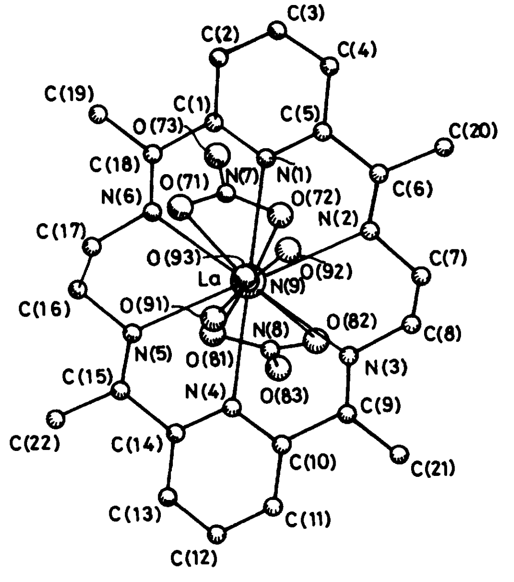

Figure 1. The molecular structure of $[La(NO_3)_3L^1]$ and atom-numbering scheme

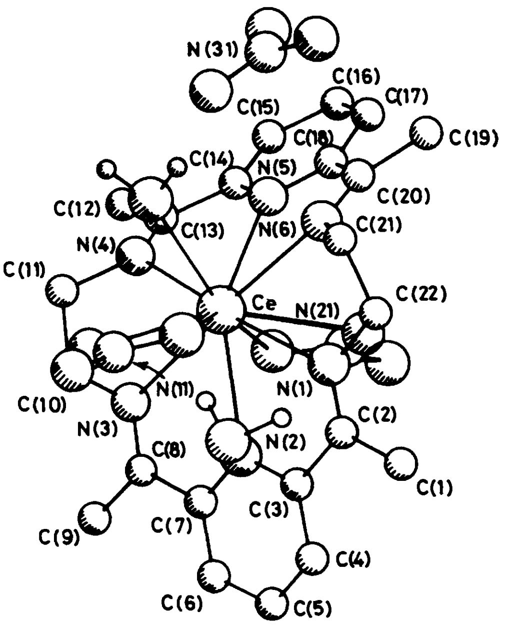

Figure 2. The molecular structure of $[Ce(NO_3)_2L^1(H_2O)]NO_3{\cdot}H_2O$ and atom-numbering scheme. The un-co-ordinated nitrate is labelled N(31) and the un-co-ordinated water is adjacent to N(2)

Structures of the Complexes.—The complex $[La(NO_3)_3L^1]$ has 12-co-ordinated La, the metal ion being co-ordinated to the six imine nitrogen atoms and to two bidentate nitrate ions on one side of the macrocycle and to the remaining nitrate ion on the other (see Figure 1). Selected bond lengths and angles are

Table 1. Selected bond lengths (Å) and angles (°) for $[La(NO_3)_3L^1]$

La–N(1)	2.746(5)	La–N(4)	2.764(5)
La–N(2)	2.672(6)	La–N(5)	2.704(6)
La–N(3)	2.729(6)	La–N(6)	2.727(7)

La–O(71)	2.767(5)	La–O(82)	2.749(5)
La–O(72)	2.730(5)	La–O(91)	2.718(5)
La–O(81)	2.705(5)	La–O(92)	2.689(5)

C(1)–N(1)	1.345(9)	C(10)–N(4)	1.346(9)
C(5)–N(1)	1.341(9)	C(14)–N(4)	1.345(10)
C(6)–N(2)	1.269(9)	C(15)–N(5)	1.276(10)
C(7)–N(2)	1.468(10)	C(16)–N(5)	1.466(11)
C(8)–N(3)	1.471(10)	C(17)–N(6)	1.481(12)
C(9)–N(3)	1.270(10)	C(18)–N(6)	1.264(10)

N(1)–La–N(2)	59.0(2)	N(2)–La–N(5)	179.4(2)
N(1)–La–N(3)	116.2(2)	N(2)–La–N(6)	116.8(2)
N(1)–La–N(4)	164.3(1)	N(3)–La–N(4)	58.7(2)
N(1)–La–N(5)	120.8(2)	N(3)–La–N(5)	116.3(2)
N(1)–La–N(6)	59.2(2)	N(3)–La–N(6)	141.6(2)
N(2)–La–N(3)	63.6(2)	N(4)–La–N(5)	58.6(2)
N(2)–La–N(4)	121.4(2)	N(4)–La–N(6)	114.2(2)
		N(5)–La–N(6)	62.9(2)

O(71)–La–N(1)	66.0(2)	O(82)–La–N(1)	121.5(2)
O(71)–La–N(2)	104.0(2)	O(82)–La–N(2)	75.2(2)
O(71)–La–N(3)	156.8(2)	O(82)–La–N(3)	63.4(2)
O(71)–La–N(4)	125.2(2)	O(82)–La–N(4)	71.1(1)
O(71)–La–N(5)	76.4(2)	O(82)–La–N(5)	96.2(2)
O(71)–La–N(6)	60.9(2)	O(82)–La–N(6)	144.2(2)
O(72)–La–N(1)	65.6(1)	O(91)–La–N(1)	99.7(2)
O(72)–La–N(2)	65.0(1)	O(91)–La–N(2)	110.7(2)
O(72)–La–N(3)	112.0(2)	O(91)–La–N(3)	76.0(2)

C(1)–C(2)	1.390(10)	C(10)–C(11)	1.395(11)
C(2)–C(3)	1.369(13)	C(11)–C(12)	1.355(13)
C(2)–C(4)	1.361(12)	C(12)–C(13)	1.374(13)
C(4)–C(5)	1.390(10)	C(13)–C(14)	1.402(11)
C(5)–C(6)	1.500(10)	C(14)–C(15)	1.486(11)
C(6)–C(20)	1.520(11)	C(15)–C(22)	1.517(13)
C(7)–C(8)	1.497(10)	C(16)–C(17)	1.494(13)
C(9)–C(10)	1.500(11)	C(18)–C(1)	1.501(11)
C(9)–C(21)	1.523(11)	C(18)–C(19)	1.521(13)

N(7)–O(71)	1.256(8)	N(8)–O(83)	1.215(8)
N(7)–O(72)	1.266(8)	N(9)–O(91)	1.256(9)
N(7)–O(73)	1.229(8)	N(9)–O(92)	1.254(8)
N(8)–O(81)	1.269(8)	N(9)–O(93)	1.224(9)
N(8)–O(82)	1.257(8)		

O(72)–La–N(4)	129.8(1)	O(91)–La–N(4)	65.0(2)
O(72)–La–N(5)	115.6(2)	O(91)–La–N(5)	68.7(2)
O(72)–La–N(6)	100.4(2)	O(91)–La–N(6)	68.2(2)
O(81)–La–N(1)	125.7(1)	O(92)–La–N(1)	64.2(2)
O(81)–La–N(2)	115.2(2)	O(92)–La–N(2)	67.0(2)
O(81)–La–N(3)	101.9(2)	O(92)–La–N(3)	69.8(2)
O(81)–La–N(4)	69.4(2)	O(92)–La–N(4)	100.9(2)
O(81)–La–N(5)	65.5(2)	O(92)–La–N(5)	112.4(2)
O(81)–La–N(6)	110.4(2)	O(92)–La–N(6)	75.6(2)

O(71)–La–O(72)	46.1(2)	O(72)–La–O(82)	62.8(1)
O(81)–La–O(82)	46.2(2)	O(72)–La–O(91)	165.1(2)
O(91)–La–O(92)	46.5(2)	O(72)–La–O(92)	122.9(2)
O(71)–La–O(81)	64.2(2)	O(81)–La–O(91)	127.1(2)
O(71)–La–O(82)	95.1(1)	O(81)–La–O(92)	169.9(2)
O(71)–La–O(91)	127.2(2)	O(82)–La–O(91)	131.2(2)
O(71)–La–O(92)	125.5(2)	O(82)–La–O(92)	129.2(2)
O(72)–La–O(81)	64.9(1)		

Least-squares planes in the form $Ax + By + Cz = D$, where x, y, z are fractional co-ordinates, with deviations (Å) of the relevant atoms

$$(6.8202)x + 5.0956y + 7.0490z = 4.2238$$

N(1)	−0.0368	C(3)	−0.0073
N(2)	0.0369	C(4)	−0.0251
N(6)	−0.0730	C(5)	−0.0382
C(1)	0.0298	C(6)	0.0219
C(2)	0.0200	C(18)	0.0718

weighted root mean square deviation,
w.r.m.s.d. = 0.0414

$$(3.7918)x + 5.6309y + 13.0185z = 3.4701$$

N(3)	−0.1230	C(11)	0.1147
N(4)	−0.0803	C(12)	0.0214
N(5)	0.1400	C(13)	−0.1072
C(9)	0.0818	C(14)	−0.1024
C(10)	0.0453	C(15)	0.0096

w.r.m.s.d. = 0.0925

Angle between normals 26.72°.

given in Table 1, together with relevant least-squares plane data. As in the case of $[La(NO_3)_3(18\text{-crown-}6)]$,[8] two nitrates are situated on one side of the macrocycle, the other on the opposite side. The two conjugated sections of the ligand are each planar and the interplanar angle is 26.7°; a considerable degree of flexibility is allowed in the ligand by the $N\text{–}CH_2\text{–}CH_2\text{–}N$ linkages. The ligand is folded away from the hemisphere containing the extra nitrate ion. La–N(pyridine) distances are 2.746(5) and 2.764(5) Å, while La–N(imine) distances are slightly shorter at 2.672(6)—2.729(6) Å (average 2.708 Å). The La–O(nitrate) distances are in the range 2.689(5)—2.767(5) Å (average 2.726 Å).

The complex ion $[Ce(NO_3)_2L^1(H_2O)]^+$ shows the unusual co-ordination number of 11. The metal ion is co-ordinated to the six ring nitrogen atoms, to one bidentate nitrate ion on one side of the macrocycle and to the remaining nitrate ion and the water molecule on the other (see Figure 2). Selected bond lengths and angles are given in Table 2, together with relevant least-squares plane data. The two coplanar conjugated sections of the ligand show a larger interplanar angle, 59.0°, than $[La(NO_3)_3L^1]$. The ligand is folded away from the hemisphere containing the extra water molecule. Ce–N(pyridine) distances are 2.637(4) and 2.726(5) Å, while Ce–N(imine) distances are slightly shorter at 2.617(5)—2.720(9) Å. There is a striking difference between the two halves of the macrocycle; one half has Ce–N at 2.722 Å (average), while the other is appreciably more closely bonded with Ce–N at 2.625 Å (average). The Ce–O(nitrate) distances are in the range 2.648(6)—2.745(5) Å (average 2.692 Å), while Ce–O(water) = 2.569(6) Å.

The complex $[\{Nd(NO_3)L^1(H_2O)_2\}_2]NO_3[ClO_4]_3\cdot4H_2O$ has 10-co-ordinated Nd, the metal ion being co-ordinated to the six ring nitrogen atoms and to one bidentate nitrate ion on one side of the macrocycle and to the two water molecules on the other (see Figure 3). Selected bond lengths and angles are given in Table 3. The two coplanar conjugated sections of the ligand show a still larger interplanar angle, 63.9°, than $[Ce(NO_3)_2L^1(H_2O)]^+$. The ligand is folded away from the hemisphere containing the two water molecules, rather than the bidentate nitrate. This is an interesting direct demonstration of the smaller steric requirements of bidentate nitrate as compared with two monodentate ligands. Nd–N(pyridine) distances are 2.614(12) and 2.628(12) Å, while Nd–N(imine) distances are

Table 2. Selected bond lengths (Å) and angles (°) for $[Ce(NO_3)_2L^1(H_2O)]NO_3 \cdot H_2O$

Ce–N(1)	2.720(9)	Ce–N(4)	2.622(8)
Ce–N(2)	2.726(5)	Ce–N(5)	2.637(4)
Ce–N(3)	2.719(6)	Ce–N(6)	2.617(5)
Ce–O(11)	2.707(8)	Ce–O(12)	2.648(6)
Ce–O(21)	2.668(7)	Ce–O(23)	2.745(5)
Ce–O(1)	2.569(5)		
C(2)–N(1)	1.270(8)	C(8)–N(3)	1.276(7)
C(13)–N(4)	1.278(8)	C(20)–N(6)	1.280(8)
C(3)–N(2)	1.362(6)	C(7)–N(2)	1.346(7)
C(14)–N(5)	1.349(7)	C(18)–N(5)	1.348(7)
C(10)–N(3)	1.475(7)	C(11)–N(4)	1.460(8)
C(21)–N(6)	1.471(8)	C(22)–N(1)	1.484(8)

C(2)–C(1)	1.504(11)	C(13)–C(12)	1.510(10)
C(3)–C(2)	1.500(8)	C(14)–C(13)	1.481(8)
C(4)–C(3)	1.389(8)	C(15)–C(14)	1.395(9)
C(5)–C(4)	1.390(9)	C(16)–C(15)	1.389(9)
C(6)–C(5)	1.391(8)	C(17)–C(16)	1.393(9)
C(7)–C(6)	1.401(8)	C(18)–C(17)	1.394(10)
C(8)–C(7)	1.504(8)	C(20)–C(18)	1.488(8)
C(9)–C(8)	1.501(10)	C(20)–C(19)	1.486(10)
C(11)–C(10)	1.501(10)	C(22)–C(21)	1.501(10)
N(11)–O(11)	1.245(7)	N(11)–O(12)	1.264(7)
N(11)–O(13)	1.231(8)		
N(21)–O(21)	1.261(7)	N(21)–O(22)	1.226(7)
N(21)–O(23)	1.242(7)		
N(31)–O(31)	1.250(8)	N(31)–O(32)	1.255(8)
N(31)–O(33)	1.224(7)		

N(1)–Ce–O(1)	114.1(3)	N(1)–Ce–O(11)	103.6(4)
N(1)–Ce–O(12)	62.3(4)	N(1)–Ce–O(21)	101.9(4)
N(1)–Ce–O(23)	62.8(4)		
N(2)–Ce–O(1)	145.5(5)	N(2)–Ce–O(11)	79.5(6)
N(2)–Ce–O(12)	78.5(4)	N(2)–Ce–O(21)	73.9(6)
N(3)–Ce–O(1)	113.1(6)	N(3)–Ce–O(11)	62.2(5)
N(3)–Ce–O(12)	102.4(6)	N(3)–Ce–O(21)	64.1(6)
N(3)–Ce–O(23)	104.6(4)		
N(4)–Ce–O(1)	74.1(6)	N(4)–Ce–O(11)	84.4(5)
N(5)–Ce–O(1)	73.5(5)	N(5)–Ce–O(11)	134.7(6)
N(6)–Ce–O(1)	71.8(6)	N(6)–Ce–O(11)	126.0(6)

O(1)–Ce–O(11)	68.8(5)	O(1)–Ce–O(12)	70.2(5)
O(1)–Ce–O(21)	136.4(6)	O(1)–Ce–O(23)	134.9(7)
O(11)–Ce–O(21)	126.3(6)	O(11)–Ce–O(23)	155.2(7)
O(12)–Ce–O(21)	152.5(5)	O(12)–Ce–O(23)	125.1(4)
O(11)–Ce–O(12)	47.2(5)	O(21)–Ce–O(23)	46.2(6)
N(1)–Ce–N(2)	59.9(6)	N(1)–Ce–N(3)	119.4(5)
N(1)–Ce–N(4)	171.5(4)	N(1)–Ce–N(5)	114.3(6)
N(1)–Ce–N(6)	61.9(6)	N(2)–Ce–N(3)	59.5(4)
N(2)–Ce–N(4)	119.9(6)	N(2)–Ce–N(5)	140.9(7)
N(2)–Ce–N(6)	120.6(4)	N(3)–Ce–N(4)	61.7(4)
N(3)–Ce–N(5)	113.9(4)	N(3)–Ce–N(6)	171.7(5)
N(4)–Ce–N(5)	59.8(8)	N(4)–Ce–N(6)	115.7(5)
N(5)–Ce–N(6)	60.2(5)		

Least-squares planes in the form $Ax + By + Cz = D$, where x, y, z are fractional co-ordinates, with deviations (Å) of the relevant atoms

$$(-0.0779)x + 6.7756y + 2.7550z = -2.5243$$

N(1)	−0.0528	C(2)	0.0332
N(2)	0.0043	C(3)	0.0192
N(3)	0.0238	C(4)	0.0283
C(5)	−0.0216	C(6)	−0.0190
C(7)	−0.0128	C(8)	−0.0027

w.r.m.s.d. = 0.0258

$$3.2068x + (-3.3240)y + 13.9630z = 11.8625$$

N(4)	−0.0526	C(15)	0.0141
N(5)	0.0821	C(16)	−0.0114
N(6)	0.0328	C(17)	−0.0394
C(13)	−0.0277	C(18)	0.0108
C(14)	0.0516	C(20)	−0.0603

w.r.m.s.d. = 0.0443

Angle between normals 58.99°.

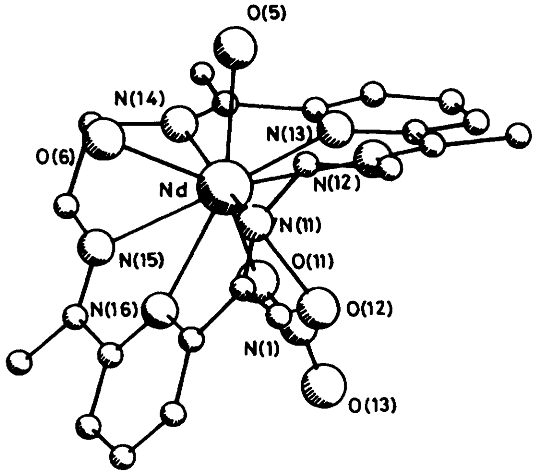

Figure 3. The molecular structure of the $[Nd(NO_3)L^1(H_2O)_2]^{2+}$ ion and atom-numbering scheme

slightly shorter at 2.573(14)—2.671(16) Å (average 2.610 Å). There is, in this instance, little difference between the two halves of the macrocycle. The Nd–O(nitrate) distances are 2.598(14) and 2.617(13) Å, while the Nd–O(water) distances are 2.493(11) and 2.516(13) Å.

In addition to the three compounds whose structures were fully determined, the other complexes of similar stoicheiometries were also examined. The 12-co-ordinate structure which is adopted by La was confirmed by single-crystal cell-dimension determinations to be adopted by Ce also. The 11-co-ordinate structure adopted by Ce was shown by similar means to be also adopted by La and Pr. Crystals of the Tb complex were similarly found to be isostructural with those of the 10-co-ordinate Nd complex, and although twinning was present in some other cases, giving difficulty with cell-dimension determination, we consider it likely on morphological grounds that the same structure is present in the series Nd, Sm, Eu, Gd, Tb, Dy, and Ho. However, single-crystal cell-dimension determination shows that the last member of this third group, Er, adopts a different crystal structure, as yet undetermined. Details of all cell dimensions appear in SUP 56674.

Table 3. Selected bond lengths (Å) and angles (°) for $[\{Nd(NO_3)L^1(H_2O)_2\}_2]NO_3[ClO_4]_3\cdot 4H_2O$*

O(11)–Nd(1)	2.598(14)	O(12)–Nd(1)	2.617(13)	C(212)–N(21)	1.250(17)	C(213)–N(21)	1.478(16)
O(5)–Nd(1)	2.516(13)	O(6)–Nd(1)	2.493(11)	C(212)–C(211)	1.531(23)	C(232)–C(212)	1.498(17)
N(11)–Nd(1)	2.584(15)	N(12)–Nd(1)	2.660(15)	C(214)–C(213)	1.536(21)	N(22)–C(214)	1.495(20)
N(13)–Nd(1)	2.614(12)	N(14)–Nd(1)	2.573(14)	C(216)–N(22)	1.283(18)	C(216)–C(215)	1.543(21)
N(15)–Nd(1)	2.671(16)	N(16)–Nd(1)	2.628(12)	C(217)–C(216)	1.499(21)	C(218)–C(217)	1.355(21)
N(1)–O(11)	1.251(15)	N(1)–O(12)	1.258(18)	N(23)–C(217)	1.336(15)	C(219)–C(218)	1.443(26)
N(1)–O(13)	1.227(17)			C(220)–C(219)	1.415(22)	C(221)–C(220)	1.414(22)
				N(23)–C(221)	1.329(18)	C(223)–C(221)	1.498(18)
C(112)–C(111)	1.514(27)	N(11)–C(112)	1.262(18)	C(223)–C(222)	1.509(24)	N(24)–C(223)	1.274(20)
C(132)–C(112)	1.464(24)	C(113)–N(11)	1.474(23)	C(224)–N(24)	1.498(17)	C(225)–C(224)	1.577(25)
C(114)–C(113)	1.532(22)	N(12)–C(114)	1.502(22)	N(25)–C(225)	1.503(21)	C(227)–N(25)	1.260(18)
C(116)–N(12)	1.254(17)	C(116)–C(115)	1.532(25)	C(227)–C(226)	1.571(23)	C(228)–C(227)	1.466(20)
C(117)–C(116)	1.510(23)	N(13)–C(117)	1.358(18)	C(229)–C(228)	1.400(18)	N(26)–C(228)	1.355(15)
C(118)–C(117)	1.402(19)	C(121)–N(13)	1.344(19)	C(230)–C(229)	1.376(21)	C(229)–C(229a)	3.472
C(119)–C(118)	1.392(27)	C(120)–C(119)	1.375(26)	C(231)–C(230)	1.373(19)	C(232)–C(231)	1.401(18)
C(121)–C(120)	1.365(19)	C(123)–C(121)	1.522(22)	N(26)–C(232)	1.350(17)		
C(123)–C(122)	1.506(25)	N(14)–C(123)	1.247(16)				
C(124)–N(14)	1.486(20)	C(125)–C(124)	1.490(23)	O(31)–N(3)	1.233(26)	O(32)–N(3)	1.191(33)
N(15)–C(125)	1.486(21)	C(127)–N(15)	1.289(20)	O(33)–N(3)	1.178(31)		
C(127)–C(126)	1.557(33)	C(128)–C(127)	1.476(22)				
C(129)–C(128)	1.363(20)	N(16)–C(128)	1.371(21)	O(1A)–Cl(1)	1.409(15)	O(2A)–Cl(1)	1.401(15)
C(130)–C(129)	1.377(24)	C(131)–C(130)	1.399(27)	O(3A)–Cl(1)	1.407(20)	O(4A)–Cl(1)	1.399(20)
C(132)–C(131)	1.412(19)	N(16)–C(132)	1.334(19)	O(1B)–Cl(2)	1.410(13)	O(2B)–Cl(2)	1.349(15)
				O(3B)–Cl(2)	1.378(22)	O(4B)–Cl(2)	1.390(26)
O(21)–Nd(2)	1.612(13)	O(22)–Nd(2)	2.639(13)				
O(7)–Nd(2)	2.494(14)	O(8)–Nd(2)	2.457(12)	O(1C)–Cl(3)	1.329(18)	O(2C)–Cl(3)	1.320(33)
N(21)–Nd(2)	2.664(13)	N(22)–Nd(2)	2.550(12)	O(3C)–Cl(3)	1.345(32)	O(4C)–Cl(3)	1.258(32)
N(23)–Nd(2)	2.631(13)	N(24)–Nd(2)	2.643(14)				
N(25)–Nd(2)	2.584(12)	N(26)–Nd(2)	2.620(12)				
O(21)–N(2)	1.287(16)	O(22)–N(2)	1.253(16)				
O(23)–N(2)	1.213(19)						
O(11)–Nd(1)–O(12)	48.6(3)	O(5)–Nd(1)–O(6)	67.3(3)	O(21)–Nd(2)–O(22)	48.6(3)	O(7)–Nd(2)–O(8)	68.0(4)
O(5)–Nd(1)–O(11)	140.8(3)	O(6)–Nd(1)–O(11)	135.9(3)	O(7)–Nd(2)–O(21)	133.9(3)	O(8)–Nd(2)–O(21)	145.9(3)
O(5)–Nd(1)–O(12)	139.5(3)	O(6)–Nd(1)–O(12)	141.0(3)	O(7)–Nd(2)–O(22)	141.3(3)	O(8)–Nd(2)–O(22)	136.0(3)
N(11)–Nd(1)–N(12)	62.5(3)	N(12)–Nd(1)–N(13)	60.7(3)	N(21)–Nd(2)–N(22)	63.4(3)	N(22)–Nd(2)–N(23)	61.3(3)
N(11)–Nd(1)–N(13)	123.2(4)	N(12)–Nd(1)–N(14)	119.8(3)	N(21)–Nd(2)–N(23)	115.9(3)	N(22)–Nd(2)–N(24)	118.9(3)
N(11)–Nd(1)–N(14)	166.1(4)	N(12)–Nd(1)–N(15)	165.9(4)	N(21)–Nd(2)–N(24)	166.5(4)	N(22)–Nd(2)–N(25)	167.7(3)
N(11)–Nd(1)–N(15)	117.9(3)	N(12)–Nd(1)–N(16)	113.5(4)	N(21)–Nd(2)–N(25)	117.1(3)	N(22)–Nd(2)–N(26)	123.0(3)
N(11)–Nd(1)–N(16)	60.6(4)			N(21)–Nd(2)–N(26)	60.0(3)		
N(13)–Nd(1)–N(14)	61.4(3)	N(14)–Nd(1)–N(15)	63.7(3)	N(23)–Nd(2)–N(24)	60.3(3)	N(24)–Nd(2)–N(25)	63.8(3)
N(13)–Nd(1)–N(15)	116.6(4)	N(14)–Nd(1)–N(16)	123.9(4)	N(23)–Nd(2)–N(25)	123.9(3)	N(24)–Nd(2)–N(26)	114.6(3)
N(13)–Nd(1)–N(16)	147.7(3)	N(15)–Nd(1)–N(16)	60.4(3)	N(23)–Nd(2)–N(26)	145.0(4)	N(25)–Nd(2)–N(26)	60.5(3)

* Key to symmetry operation relating designated atom to reference atoms at (x, y, z): (a) $1.0 - x$, $1.0 - y$, $1.0 - z$.

These three structures adopted by the metals La—Ho show decreasing co-ordination numbers, namely 12, 11, and 10. The smallest lanthanides clearly have too small ionic radii to co-ordinate predominantly with the macrocyclic ligand in competition with barium, and furthermore they do not form a suitably sized template for condensation of the components of the macrocycle. These two circumstances, which are shown by the failure of both the ligand replacement and the template synthetic methods, are clearly inter-related. The early lanthanides seem in these complexes to be on the 12 to 11 co-ordination borderline, and accept compact bidentate nitrate ligands in non-aqueous solution to give a co-ordination number of 12, while in aqueous solution the overall effect is to substitute a co-ordinated bidentate nitrate ion by a monodentate water molecule. A further noticeable effect is the non-coplanarity of the macrocycle, which increases in the sequence 12 ⟶ 11 ⟶ 10 co-ordination and thus seems to be a result of the ligand buckling in order to retain hexadentate contact with the smaller ions, rather than being the result of different steric requirements of the ligands on either side of the macrocycle. These steric requirements are in no case too dissimilar but are at their most dissimilar in $[La(NO_3)_3L^1]$ which has the smallest interplanar angle. However, these unbalanced steric requirements do determine the direction, though not the extent, of the folding.

N.M.R. Studies.—The n.m.r. spectra of these complexes are of interest. The ^1H spectra were obtained at 60, 80, or 400 MHz in D_2O. The species present in water will be $[ML^1(D_2O)_n]^{3+}$, where n is unknown but is possibly 3 or 4 and may well alter as the lanthanide series is traversed. Spectra were obtained for M = La, Ce, Pr, Nd, Sm, Gd, Tb, Dy, Ho, and Er.

Lanthanide n.m.r. spectra may be analysed on the basis that the observed paramagnetic shifts are caused by a combination of a dipole–dipole interaction and a contact interaction. Usually the dipolar interaction predominates. Where a series of isostructural lanthanide complexes is present, the two contributions may be separated because for any individual lanthanide at constant temperature, the paramagnetic shift $\Delta H/H$ is given by equation (1). Here C is the geometrical

$$\Delta H/H = C \cdot A + C'\langle S_z\rangle \qquad (1)$$

parameter and C' is the hyperfine spin–spin coupling constant; both of course are different for each nucleus. $\langle S_z \rangle$ is the average resolved part of the electron spin in the z direction, and A is Bleaney's constant.[9] ΔH is in this work operationally defined as the upfield movement in the chemical shift of a certain nucleus in a paramagnetic lanthanide complex when compared with the chemical shift of the corresponding nucleus of the corresponding La complex. If the hyperfine coupling constant is assumed invariant from lanthanide to lanthanide, shift data from two or more isostructural complexes will suffice to apportion the total shift as between the dipolar portion $C \cdot A$ and the contact portion $C'\langle S_z \rangle$.

The observed ^1H shifts are shown in Table 4. Assignments are straightforward for the lighter lanthanides, on the basis of chemical shift, integration, and coupling. The Gd spectrum showed one very broad line only. In the post-Gd complexes, the CH_2 resonance, already very broad in the series Ce—Eu, was not observed. However, except for the Er complex, integration allowed assignment of the other proton resonances. For the very broadened spectrum of the Er complex, the assignments given in Table 4 must be regarded as uncertain.

The shift values (relative to the lanthanide complex) were analysed as two series: Ce—Nd and Tb—Er. The spectra of the Sm, Eu, and Gd complexes are unsuitable for this purpose and were omitted. The shifts were fitted for least-squares deviation from equation (1), when the series Ce—Nd gave a satisfactory fit for the values of C and C' shown in Table 4. The root sums of squares of the deviations from observed shift values were 0.18, 0.03, 1.61, and 0.47 p.p.m. for the β-pyridine, γ-pyridine, CH_2, and CH_3 protons respectively. For the series Tb—Er, however, fits were very poor as could indeed be forecast by inspection of values of A, $\langle S_z \rangle$, and the observed shifts. If the values of C and C' obtained for Ce—Nd are used, a rather poor fit (average deviation, 8.30 p.p.m.) is obtained for Tb, but Dy, Ho, and Er give no reasonable fit at all (average deviations, 14.15, 18.82, and 14.29 p.p.m. respectively). It is likely, therefore, that a change of structure in solution occurs on traversing the series Tb—Er and has already substantially begun by the time Tb is reached. It cannot be ascertained whether the structural change is by means of an n.m.r.-rapid equilibrium between two or more distinct structures which is progressively displaced as the series is traversed, or whether only one structure is present for each metal ion, but progressively alters with ionic radius. The crystal structures reported herein must be treated with caution as predictors of the structures in solution. However, they do suggest that a progressive structural change involving an increasing dihedral angle between the two approximately coplanar halves of the macrocycle probably does take place with decreasing ionic radius, occurring to some extent even in the first part of the lanthanide series where the shifts fit equation (1) well.

Table 4. ^1H N.m.r. spectra of the lanthanide complexes of L^1 in D_2O at probe temperature. δ Values are in p.p.m. relative to sodium 3-trimethylsilylpropane-1-sulphonate; values in parentheses are band widths at half height in Hz. Spectra are at 80 MHz except Nd and Sm which are at 400 MHz. In the cases of La, Sm, and Er the pyridine (py) resonances coincided. As explained in the text, C and C' were calculated from the paramagnetic shifts of the Ce, Pr, and Nd compounds only

	δ_H/p.p.m.			
M	β-py	γ-py	CH_2	CH_3
La	8.21(2)	8.21(2)	4.04(4)	2.59(2)
Ce	13.04(4)	12.18(4)	0.74(9)	3.79(4)
Pr	18.13(4)	15.63(4)	3.92(12)	6.60(4)
Nd	13.81(35)	11.70(15)	11.88(40)	5.35(15)
Sm	8.91(2)	8.91(2)	3.34(3)	3.18(3)
Eu	1.07(4)	4.52(4)	−7.60(8)	−0.05(3)
Gd	One very broad signal at *ca.* 5			
Tb	49.62(90)	39.06(120)		17.04(75)
Dy	75.63(120)	70.74(120)		28.81(120)
Ho	41.86(75)	32.85(75)	−0.96(200)	31.56(85)
Er	−16.09(50)	−16.09(50)		22.80(75)
C	0.389	0.319	−0.400	0.113
C	−0.560	−0.224	−2.517	−0.438

The values of C' decrease in magnitude in the sequence −2.52 (three-bond interaction), −0.56 and −0.44 (four bonds), and −0.22 (five bonds), and this seems reasonable provided the f delocalisation is by means of σ bond interaction. The values of C strongly suggest a predominant cos 2θ dependence where θ is the azimuthal angle in the (buckled) pseudo-plane of the macrocycle. We have earlier discussed the relation of the magnetic anisotropy tensor to the geometry of co-ordinated macrocycles in the presence of conformational and co-ordination equilibria in the case of a praseodymium complex of a substituted crown ether.[10] In the present series there are not enough different protons in the macrocycle to make possible a soundly based determination of the unknown geometrical parameters (ligand fold angle, even if assumed constant, and anisotropy tensor orientation) and the unknown magnetic anisotropy parameters ($\chi_x - \chi_y$ and $\chi_z - \bar{\chi}$).

It is noteworthy that the Pr oxygen-donor crown ether complex showed little evidence of a contact mechanism for proton shifts,[10] while the nitrogen-donor macrocycle which is the subject of the present study shows fairly considerable proton contact shifts in addition to the dipolar mechanism which is on the whole predominant.

The ^{13}C spectra of the La, Ce, and Pr compounds were obtained from D_2O solutions. The Pr spectrum had broadened signals and a noisy baseline. Assignments of the La spectrum were made by comparison with reported spectra of pyridine, 2,6-diacetylpyridine, 2,6-diacetylpyridine bis(4-methoxybenzoylhydrazone), and 2,6-diacetylpyridine (2′-pyridylhydrazone) (4″-methoxybenzoylhydrazone)[11–13] and from intensity considerations. The assignments for Ce and Pr followed by comparison with the La spectrum. All are listed in Table 5; the assignments for the 2,6-pyridyl and the imine carbon atoms might be interchanged but would then give highly abnormal paramagnetic shifts. The ^{13}C paramagnetic shifts have been fitted to equation (1) and give values of C and C' as shown (Table 5). The sensitivity of the fits for the particular values of A and $\langle S_z \rangle$ which apply to Ce and Pr is unfortunately quite coarse and hence excellent fits are obtained for the values of C and C' in Table 5 which are given to only one decimal place. The C' values indicate relatively high contact contributions to the total paramagnetic shifts. These contributions lie within the wide range 8—81%, depending on the geometry-controlled magnitude of the dipolar component as well as on the magnitude of the contact component, but these values are not precise and any attempt to correlate the values of C' with the bonding situations of individual carbon atoms would probably be unsound.

Table 5. ^{13}C N.m.r. spectra of the lanthanide complexes of L^1 in D_2O at probe temperature. δ Values are in p.p.m. relative to 1,4-dioxane as reference (δ 66.5 p.p.m.)

	δ_C/p.p.m.					
M	$C^{2,6}$(py)	$C^{3,5}$(py)	C^4(py)	CH_3	C=N	CH_2
La	154.5	126.7	142.0	15.9	171.8	52.0
Ce	175.3	136.6	148.3	23.8	181.5	46.1
Pr	193.6	148.7	152.6	37.5	193.6	46.7
C	1.6	0.5	0.6	0.2	0.5	−1.0
C'	−2.0	−3.9	0.6	−5.9	−3.9	−5.0

The complex $[Ce(NO_3)_3L^1]$ was tested in aqueous solution as a shift reagent. On addition of acetate ion at an acetate:complex ratio of 9:1 the acetate proton resonance showed an upfield shift of 0.68 p.p.m., while a ratio of 2.1:1 (0.092 mol dm^{-3} acetate and 0.043 mol dm^{-3} complex) increased the shift to 2.49 p.p.m. The different ligand fields produced by the macrocycle and by the water and acetate ligands which undoubtedly co-ordinate above and below the 'plane' of the buckled macrocyclic hexaimine evidently lead to a magnetic anisotropy which produces the observed acetate shifts. The complex produced no shifts in the proton resonances of added pyridine, very probably due to a low association constant for this ligand.

Experimental

Lanthanide oxides, analyses, i.r. spectra, n.m.r. spectra, thermogravimetric data, and conductance data were obtained as described previously.[8]

Preparations.—$[La(NO_3)_3L^1]$. 2,6-Diacetylpyridine (0.245 g, 1.5 mmol) was dissolved in a solution of anhydrous ethylenediamine (0.088 g, 1.5 mmol) in methanol (10 cm^3). The resulting solution was added to a solution of hydrated lanthanum nitrate (0.33 g, 0.76 mmol) in methanol (20 cm^3). The mixture, which immediately became orange, was refluxed for 4 h, during which

Table 6. Analytical data

	Analysis* (%)		
M	C	H	N
(*a*) $[M(NO_3)_3L^1]$			
La	37.5 (37.8)	3.9 (3.75)	17.7 (18.0)
Ce	37.7 (37.7)	3.8 (3.7)	17.6 (18.0)
(*b*) $[M(NO_3)_2L^1(H_2O)]NO_3{\cdot}H_2O$			
La	36.1 (35.9)	4.1 (4.1)	17.2 (17.1)
Cc	36.1 (35.9)	4.1 (4.1)	17.1 (17.1)
Pr	36.1 (35.8)	4.1 (4.1)	17.4 (17.1)
(*c*) $[\{M(NO_3)L^1(H_2O)_2\}_2]NO_3[ClO_4]_3{\cdot}4H_2O$			
Nd	31.9 (31.7)	4.0 (4.1)	12.7 (12.6)
Sm	31.4 (31.5)	4.0 (4.1)	12.8 (12.5)
Eu	31.5 (31.4)	3.8 (4.1)	13.0 (12.5)
Gd	31.5 (31.2)	4.0 (4.05)	13.0 (12.4)
Tb	31.2 (31.2)	4.1 (4.0)	12.6 (12.4)
Dy	30.6 (31.0)	3.9 (4.0)	12.6 (12.3)
Ho	31.3 (30.95)	3.9 (4.0)	12.65 (12.3)
Er	31.3 (30.9)	4.0 (4.0)	12.9 (12.3)

* Calculated values are given in parentheses.

Table 7. *X*-Ray data for $[La(NO_3)_3L^1]$, $[Ce(NO_3)_2L^1(H_2O)]NO_3{\cdot}H_2O$, and $[\{Nd(NO_3)L^1(H_2O)_2\}_2]NO_3[ClO_4]_3{\cdot}4H_2O$

	$[La(NO_3)_3L^1]$ $C_{22}H_{26}LaN_9O_9$	$[Ce(NO_3)_2L^1(H_2O)]NO_3{\cdot}H_2O$ $C_{22}H_{30}CeN_9O_{11}$	$[\{Nd(NO_3)L^1(H_2O)_2\}_2]NO_3[ClO_4]_3{\cdot}4H_2O$ $C_{44}H_{68}Cl_3N_{15}Nd_2O_{29}$
(*a*) Crystal data			
M	699.40	736.65	1521.69
a/Å	8.623(1)	8.961(4)	11.970(1)
b/Å	18.221(2)	9.079(2)	14.880(2)
c/Å	17.039(2)	18.247(3)	19.678(3)
α/°		86.12(1)	72.11(2)
β/°	99.01(2)	103.66(2)	76.58(3)
γ/°		100.63(3)	86.55(2)
U/Å³	2 644.2	1 417.3	3 244.15
Space group	$P2_1/c$	$P\bar{1}$	$P\bar{1}$
D_m/g cm^{-3}	1.73	1.74	1.6
Z	4	2	2
D_c/g cm^{-3}	1.75	1.82	1.64
F(000)	1 400	742	1 680
$\mu(Mo\text{-}K_\alpha)/cm^{-1}$	15.55	1.47	16.38
(*b*) Data collection			
Crystal size/mm	0.35 × 0.25 × 0.20	0.65 × 0.27 × 0.25	0.55 × 0.38 × 0.33
$\theta_{min.}$, $\theta_{max.}$/°	1.5, 26	1.5, 28	1.5, 25
Scan width parameters *A*,*B* in width = *A* + *B*tanα	0.8, 0.35	0.8, 0.35	0.8, 0.35
Horizontal aperture parameters *A*,*B* in aperture = *A* + *B*tanθ	4.0, 0.0	4.0, 0.0	4.0, 0.0
Total unique data	5 114	3 930	7 863
Observed data	3 453	3 478	5 397
Significance test	$I > 1.5\sigma(I)$	$I > 1.5\sigma(I)$	$I > 3\sigma(I)$
(*c*) Refinement			
No. of parameters	435	470	593
Weighting scheme coefficient *g* in $w = 1/[\sigma^2(F_o) + g(F_o)^2]$	unit weights	0.0001	0.0007
Final *R* $(= \Sigma\Delta F/\Sigma\lvert F_o\rvert)$	0.036	0.037	0.062
R' $\{= [\Sigma(w\Delta F^2)/\Sigma(wF_o^2)]^{\frac{1}{2}}\}$	0.043	0.035	0.064

Table 8. Atomic co-ordinates (× 10^4) for $[La(NO_3)_3L^1]$

Atom	*x*	*y*	*z*	Atom	*x*	*y*	*z*
La	3 115(0.4)	2 469(0.2)	383(0.2)	C(15)	1 473(9)	1 262(4)	1 698(4)
N(1)	3 129(6)	3 946(3)	60(3)	C(16)	510(10)	2 476(6)	1 822(5)
N(2)	4 733(6)	3 002(3)	−705(3)	C(17)	1 492(11)	3 135(5)	2 076(5)
N(3)	5 736(6)	1 707(3)	162(4)	C(18)	1 923(9)	4 141(4)	1 240(5)
N(4)	3 741(6)	1 094(3)	1 041(3)	C(19)	1 294(11)	4 695(5)	1 779(5)
N(5)	1 501(7)	1 937(3)	1 498(3)	C(20)	5 212(9)	3 876(5)	−1 746(4)
N(6)	2 073(8)	3 461(4)	1 381(4)	C(21)	7 673(10)	683(5)	396(6)
C(1)	2 424(7)	4 424(4)	491(4)	C(22)	392(11)	932(5)	2 226(5)
C(2)	2 134(9)	5 143(4)	238(5)	N(7)	148(6)	3 109(3)	−763(4)
C(3)	2 626(10)	5 377(4)	−446(6)	O(71)	154(6)	3 073(3)	−27(3)
C(4)	3 392(9)	4 902(4)	−869(5)	O(72)	1 340(5)	2 861(3)	−1 024(3)
C(5)	3 637(7)	4 179(4)	−602(4)	O(73)	−958(6)	3 378(3)	−1 214(4)
C(6)	4 551(7)	3 638(4)	−1 010(4)	N(8)	1 363(7)	1 255(3)	−762(4)
C(7)	5 705(8)	2 452(5)	−1 029(4)	O(81)	798(6)	1 517(3)	−177(3)
C(8)	6 714(8)	2 079(4)	−351(5)	O(82)	2 747(5)	1 442(3)	−812(3)
C(9)	6 155(8)	1 088(3)	465(4)	O(83)	626(7)	849(3)	−1 250(3)
C(10)	5 029(8)	718(4)	925(4)	N(9)	5 833(8)	2 968(4)	1 722(4)
C(11)	5 280(11)	4(5)	1 214(5)	O(91)	4 912(6)	2 462(3)	1 844(3)
C(12)	4 216(11)	−333(5)	1 598(5)	O(92)	5 711(7)	3 204(3)	1 024(3)
C(13)	2 902(11)	53(5)	1 715(5)	O(93)	6 802(7)	3 231(4)	2 249(4)
C(14)	2 713(9)	783(4)	1 458(4)				

Table 9. Atomic co-ordinates (× 10^4) for $[Ce(NO_3)_2L^1(H_2O)]NO_3{\cdot}H_2O$

Atom	*x*	*y*	*z*	Atom	*x*	*y*	*z*
Ce	3 678(0.3)	444(0.2)	2 477(0.1)	C(16)	8 759(7)	−3 249(7)	5 711(3)
N(1)	8 498(5)	1 689(4)	8 340(2)	C(17)	9 390(6)	−1 763(7)	5 893(3)
N(2)	6 692(4)	−406(4)	9 049(2)	C(18)	8 621(6)	−1 003(6)	6 287(3)
N(3)	4 418(4)	−2 423(4)	8 229(2)	C(19)	10 592(8)	1 371(9)	6 225(5)
N(4)	4 553(5)	−2 735(4)	6 768(2)	C(20)	9 187(5)	599(6)	6 482(3)
N(5)	7 293(4)	−1 655(4)	6 486(2)	C(21)	8 772(7)	2 725(6)	7 092(3)
N(6)	8 401(5)	1 152(5)	6 862(2)	C(22)	9 459(7)	2 792(7)	7 926(3)
C(1)	9 930(10)	2 958(10)	9 516(5)	O(1)	4 893(4)	516(4)	6 240(2)
C(2)	8 752(6)	1 779(6)	9 052(3)	O(2)	6 433(6)	4 135(5)	8 875(2)
C(3)	7 812(6)	627(5)	9 467(3)	O(11)	3 582(5)	304(4)	7 608(2)
C(4)	8 108(6)	615(6)	10 249(3)	O(12)	5 485(4)	2 141(4)	7 687(2)
C(5)	7 251(7)	−489(7)	10 624(3)	O(13)	3 222(5)	2 537(5)	7 781(3)
C(6)	6 096(6)	−1 545(6)	10 204(3)	N(11)	4 068(6)	1 672(6)	7 691(2)
C(7)	5 855(6)	−1 456(5)	9 417(3)	O(21)	7 362(4)	−2 961(4)	8 067(2)
C(8)	4 597(6)	−2 562(5)	8 944(3)	O(22)	9 729(5)	−3 349(4)	8 466(2)
C(9)	3 619(7)	−3 764(6)	9 317(3)	O(23)	9 240(4)	−1 134(4)	8 090(2)
C(10)	3 217(7)	−3 536(7)	7 767(3)	N(21)	8 812(5)	−2 492(5)	8 208(2)
C(11)	3 020(6)	−3 103(7)	6 946(3)	O(31)	6 137(5)	2 567(4)	5 273(2)
C(12)	4 299(9)	−5 205(7)	6 207(5)	O(32)	7 389(5)	1 159(5)	4 806(2)
C(13)	5 104(6)	−3 639(5)	6 440(3)	O(33)	8 328(5)	3 478(5)	5 008(3)
C(14)	6 652(6)	−3 070(3)	6 274(3)	N(31)	7 285(5)	2 406(5)	5 029(2)
C(15)	7 355(6)	−3 910(6)	5 885(3)				

time crystals of the product formed. After cooling and allowing to stand overnight, the pale pink-brown product was collected by filtration, washed with a little cold methanol, and air-dried. Yield: 0.32 g (61%). The corresponding deep yellow cerium complex was obtained similarly in 46% yield.

$[La(NO_3)_2L^1(H_2O)]NO_3{\cdot}H_2O$. To a solution of $La(NO_3)_3{\cdot}6H_2O$ (0.45 g, 1.04 mmol) in water (1.6 cm^3) in a thin (8-mm internal diameter) glass tube was added finely powdered $[Ba(ClO_4)_2L^1]$ (0.1 g, 0.14 mmol). The mixture was shaken and then allowed to remain for 24 h with the stoppered tube horizontal. The colourless crystalline product was collected by filtration, washed successively with a little cold water, and when fairly dry, with a little diethyl ether. The crystals were air-dried. Yield: 0.08 g (78%). The corresponding orange cerium and pale green praseodymium complexes were prepared similarly in 65—85% yield.

$[\{Nd(NO_3)L^1(H_2O)_2\}_2]NO_3[ClO_4]_3{\cdot}4H_2O$. When the method described immediately above for the La, Ce, and Pr complexes was applied to neodymium, the lilac perchlorate nitrate complex was obtained. Yield: 0.08 g (69%). In the same way, the corresponding cream samarium, colourless europium, gadolinium, terbium, and dysprosium, pale yellow holmium, and pale pink erbium complexes were prepared in 50—75% yields. Analytical data for all the complexes are given in Table 6.

X-Ray Crystallography.—Crystals of all three compounds, which were air-stable, were mounted on glass fibres for *X*-ray study. Preliminary cell dimensions were obtained photographically and accurate values by least-squares refinement of diffractometer setting angles (25 reflections in the range $11 < 2\theta < 18°$ in each case). Intensity data were recorded as previously described,[14] corrected for Lorentz polarisation factors but not for absorption. The structures were solved by the heavy-atom method and refined by least squares. For the La and Ce complexes, non-hydrogen atoms were refined anisotropically, and hydrogen atoms isotropically with experimentally

Table 10. Atomic co-ordinates (× 10^4) for $[\{Nd(NO_3)L^1(H_2O)_2\}_2]NO_3[ClO_4]_3{\cdot}4H_2O$

Atom	*x*	*y*	*z*	Atom	*x*	*y*	*z*
Nd(1)	2 051(1)	2 675(1)	2 367(0.5)	O(2C)	8 344(23)	2 155(18)	4 296(14)
N(1)	3 103(9)	965(8)	1 956(6)	O(3C)	7 618(22)	1 045(19)	3 963(14)
O(11)	2 495(8)	1 523(7)	1 581(5)	O(4C)	6 556(28)	1 914(21)	4 333(17)
O(12)	3 370(8)	1 194(7)	2 463(5)	Nd(2)	5 241(1)	7 441(1)	2 573(0.5)
O(13)	3 445(9)	228(7)	1 828(5)	N(2)	4 611(10)	5 830(8)	2 064(6)
O(5)	2 177(8)	4 401(7)	2 247(5)	O(21)	5 619(8)	6 213(6)	1 843(5)
O(6)	286(8)	3 251(7)	3 058(5)	O(22)	3 883(8)	6 169(6)	2 485(5)
C(111)	2 806(16)	1 093(13)	4 782(10)	O(23)	4 406(9)	5 178(7)	1 861(5)
C(112)	2 289(12)	1 428(10)	4 115(7)	O(7)	6 199(8)	7 813(8)	3 455(5)
N(11)	2 460(9)	2 243(9)	3 661(6)	O(8)	5 113(9)	9 124(6)	2 492(5)
C(113)	3 186(13)	2 970(11)	3 720(8)	N(21)	7 201(8)	6 505(8)	2 638(5)
C(114)	4 358(13)	2 948(11)	3 206(8)	C(211)	8 245(14)	4 992(12)	2 888(8)
N(12)	4 142(9)	3 054(8)	2 463(6)	C(212)	7 224(11)	5 648(9)	2 985(7)
C(115)	6 234(14)	3 370(11)	1 935(8)	C(213)	8 243(12)	6 934(10)	2 086(7)
C(116)	4 981(12)	3 233(10)	1 923(8)	C(214)	8 075(12)	8 002(10)	1 784(7)
C(117)	4 731(11)	3 384(9)	1 178(7)	N(22)	6 973(9)	8 110(7)	1 533(6)
N(13)	3 599(9)	3 409(7)	1 167(6)	C(215)	8 014(15)	8 631(12)	207(9)
C(118)	5 619(13)	3 534(11)	548(8)	C(216)	6 952(11)	8 371(9)	851(7)
C(119)	5 258(16)	3 779(13)	−109(10)	C(217)	5 793(11)	8 471(9)	670(6)
C(120)	4 116(13)	3 850(11)	−132(8)	C(218)	5 704(13)	8 763(11)	−38(8)
C(121)	3 312(11)	3 644(9)	514(7)	C(219)	4 558(15)	8 848(12)	−167(9)
C(122)	1 686(15)	4 078(12)	−181(9)	C(220)	3 596(14)	8 684(11)	432(8)
C(123)	2 029(12)	3 704(10)	543(7)	C(221)	3 850(11)	8 412(9)	1 134(7)
N(14)	1 386(9)	3 444(8)	1 167(6)	N(23)	4 906(8)	8 278(6)	1 250(5)
C(124)	115(13)	3 424(11)	1 281(8)	C(222)	1 664(14)	8 471(12)	1 693(9)
C(125)	−256(14)	2 413(12)	1 561(8)	C(223)	2 877(12)	8 276(10)	1 793(7)
N(15)	196(9)	1 906(9)	2 218(6)	N(24)	3 169(9)	8 041(7)	2 406(6)
C(126)	−935(17)	469(14)	2 376(10)	C(224)	2 209(12)	7 930(10)	3 070(7)
C(127)	−120(14)	1 052(12)	2 598(8)	C(225)	2 761(13)	7 805(10)	3 746(8)
C(128)	373(12)	585(10)	3 238(7)	N(25)	3 616(9)	7 023(8)	3 746(6)
C(129)	83(13)	−313(11)	3 675(8)	C(226)	2 188(16)	5 878(13)	4 685(10)
C(130)	556(13)	−688(11)	4 276(8)	C(227)	3 390(12)	6 187(11)	4 151(7)
C(131)	1 298(13)	−134(11)	4 440(8)	C(228)	4 292(11)	5 486(9)	4 091(7)
C(132)	1 558(11)	791(10)	3 965(7)	C(229)	4 185(12)	4 553(10)	4 551(7)
N(16)	1 110(9)	1 142(8)	3 378(6)	C(230)	5 097(12)	3 953(10)	4 482(7)
Cl(1)	1 161(4)	6 313(3)	835(3)	C(231)	6 103(12)	4 276(10)	3 979(7)
O(1A)	442(11)	7 103(10)	699(8)	C(232)	6 156(11)	5 217(9)	3 533(6)
O(2A)	554(13)	5 585(11)	1 418(9)	N(26)	5 269(9)	5 817(7)	3 583(5)
O(3A)	2 154(12)	6 561(14)	1 006(9)	N(3)	6 820(16)	974(17)	1 575(10)
O(4A)	1 534(13)	6 015(13)	211(9)	O(31)	7 392(16)	1 646(13)	1 119(10)
Cl(2)	8 984(3)	6 935(3)	4 037(2)	O(32)	7 028(16)	192(13)	1 545(11)
O(1B)	9 232(14)	7 707(10)	3 393(7)	O(33)	6 027(20)	1 124(16)	2 006(13)
O(2B)	7 847(12)	6 740(13)	4 231(8)	O(1)	444(17)	4 236(14)	4 012(10)
O(3B)	9 430(15)	7 161(12)	4 551(9)	O(2)	5 011(14)	8 724(13)	4 383(9)
O(4B)	9 607(20)	6 173(17)	3 885(12)	O(3)	5 401(21)	638(17)	3 565(12)
Cl(3)	7 581(6)	1 943(4)	3 980(3)	O(4)	9 058(23)	834(18)	147(14)
O(1C)	7 809(15)	2 503(13)	3 291(10)				

determined positions. For the Nd complex, only the Nd atom, the N atoms of the macrocycle, all atoms of the NO_3 groups, and Cl and O atoms of some of the ClO_4 groups were refined anisotropically. All other atoms, including hydrogens, which were located experimentally, were refined isotropically. A summary of the crystal data, intensity measurement parameters, and refinement details is given in Table 7. Atomic co-ordinates are given in Tables 8, 9, and 10. Details of computers, programs, and scattering-factor data are given in ref. 14.

Acknowledgements

We thank the S.E.R.C. for their support of this work.

References

1 J. D. J. Backer-Dirks, C. J. Gray, F. A. Hart, M. B. Hursthouse, and B. C. Schoop, *J. Chem. Soc., Chem. Commun.*, 1979, 774.
2 W. Radecka-Paryzek, *Inorg. Chim. Acta*, 1980, **45**, L147.
3 K. K. Abid, D. E. Fenton, U. Casellato, P. A. Vigato, and R. Graziani, *J. Chem. Soc., Dalton Trans.*, 1984, 351.
4 K. K. Abid and D. E. Fenton, *Inorg. Chim. Acta*, 1984, **95**, 119.
5 W. Radecka-Paryzek, *Inorg. Chim. Acta*, 1985, **109**, L21.
6 J. de O. Cabral, M. F. Cabral, W. J. Cummins, M. G. B. Drew, A. Rodgers, and S. M. Nelson, *Inorg. Chim. Acta*, 1978, **30**, L313.
7 F. A. Hart and F. P. Laming, *J. Inorg. Nucl. Chem.*, 1964, **26**, 579.
8 J. D. J. Backer-Dirks, J. E. Cooke, A. M. R. Galas, J. S. Ghotra, C. J. Gray, F. A. Hart, and M. B. Hursthouse, *J. Chem. Soc., Dalton Trans.*, 1980, 2191.
9 B. Bleaney, *J. Magn. Reson.*, 1972, **8**, 91.
10 G. A. Catton, M. E. Harman, F. A. Hart, G. E. Hawkes, and G. P. Moss, *J. Chem. Soc., Dalton Trans.*, 1978, 181.
11 R. J. Pugmire and D. M. Grant, *J. Am. Chem. Soc.*, 1968, **90**, 697.
12 G. Paolucci, G. Marangoni, G. Bandoli, and D. A. Clement, *J. Chem. Soc., Dalton Trans.*, 1980, 1304.
13 G. Marangoni and G. Paolucci, *J. Chem. Soc., Dalton Trans.*, 1981, 357.
14 M. B. Hursthouse and K. M. A. Malik, *J. Chem. Soc., Dalton Trans.*, 1978, 1334.

Received 21*st May* 1986; *Paper* 6/988